All Fiber Interferometer for Ice Detection

J.A. Arozarena-Arana[1], A.B. Socorro-Leránoz[1,2,*], I. Del Villar[1,2], S. Díaz[1,2], I.R. Matías[1,2]
[1]*UPNA Sensors Group, Department of Electrical and Electronic Engineering, Ed. Los Tejos*
[2]*Institute of Smart Cities, R&D Center in Communications Electronics Jerónimo de Ayanz*
Public University of Navarre, Campus of Arrosadía s/n, 31006 Pamplona, Navarre, Spain
[*]*ab.socorro@unavarra.es*

Abstract: This work presents an etched single-mode – multimode – single-mode structure that detects the solid-to-liquid change of state of the water due to an increased refractive index sensitivity within the 1.308 – 1.321 RIU range.
OCIS codes: (010.2940) Ice crystal phenomena; (010.7340) Water; (060.2370) Fiber optics sensors; (120.3180) Interferometry; (290.3030) Index measurements.

1. Introduction

In recent years, optical fiber sensors have attracted tremendous attention due to their benefits, for instance, in biochemical sensing or security monitoring [1,2]. Numerous advantages support this increasing interest, such as its reduced size, immunity to electromagnetic interferences, remote sensing capability or high sensitivity [3].

The motivation for conducting this experiment is to alert the formation of ice on the wings of airplanes and thus increase safety in air transport. Moreover, there are many applications where an ice detector sensor is crucial to guarantee a correct performance of the machines, among them, the formation of ice either on the wings of helicopters or aircrafts or on wind turbine blades [4-6].

In the domain of ice detection there are some examples where optical fiber sensors have been used. In [7] a Fabry-Perot fiber-optic interferometer is manufactured using a hollow-core photonic crystal fiber (HCPCF) fused to a single-mode fiber (SMF). This sensor responds to temperature when introduced into a liquid. Other contributions present an optofluidic detection by coupling the light from an SMF to an HCPCF or by exciting certain modes using photonic crystal fibers (PCF), with a sensitivity to temperature of 45 pm/°C [8]. Finally, in [9], PCFs are first filled with ethanol and then fused to an SMF fiber. The experimental results show that the fully ethanol-filled fibers have a thermal sensitivity up to 292 pm/°C, whereas in the case of the partially ethanol-filled the change is 120 pm/°C.

This contribution will address ice detection from a refractive index point of view. For this purpose, an interferometric structure will be used, consisting of an etched single-mode – multimode – single-mode structure (E-SMS). Then, a characterization of both the temperature detection and ice formation will be shown, in order to figure out the differences between detecting temperature and detecting freezing. Finally, some conclusions will be extracted on the use of this simple detection platform as an ice detector.

2. Experimental details

2.1. Manufacturing of the fiber-optic interferometer

The optical sensor designed for the detection of ice is an etched single-mode – multimode – single-mode structure (E-SMS) and it is shown in Fig. 1. Briefly, it is a basic interferometer consisting of a 15-mm length coreless fiber segment spliced between two single mode fibers, to form a waveguide of total diameter 125 μm.

The inherent sensitivity to refractive index variations of this device is 162 nm/RIU [10]. However, this value can be even improved with a diameter reduction using hydrofluoric acid from 125 μm to 30 μm [11]. This gives the sensor an increased capability of detecting refractive index variations at the same time the transmission and attenuation bands showing up in the spectrum give higher resolution due to their reduced bandwidth. Taking advantage of these properties, the detection of water freezing and temperature decrease will be addressed.

Once the sensor has been prepared, it is fixed to a glass frame, also fixed inside a plastic container to have the fibers straight and to avoid the deformation and torsion of the cables. The plastic container is slightly filled with purified water, so that the sensor is just submerged within it.

2.2. Description of the monitoring set-up

So as to arrange our assembly, a freezer with a couple of wall passages was conveniently prepared to pass all the necessary cables outside the freezing cabin. A white light SLED source (Agilent 83437A) was connected to one side of the sensor and an optical spectrum analyzer (Agilent 86140A OSA) was connected to the other. In addition, a Pt100 probe was also introduced inside the water to measure the electronic variation of the temperature along the duration of the experiments. The Pt100 resistor value was monitored using an Arduino-based configuration, what helped translate the resistor values into temperature values by means of software. Therefore, the freezer generated the optimal conditions to simulate a cooling climatic chamber, at the same time that a simultaneous monitoring of both the temperature and the wavelength shift could take place.

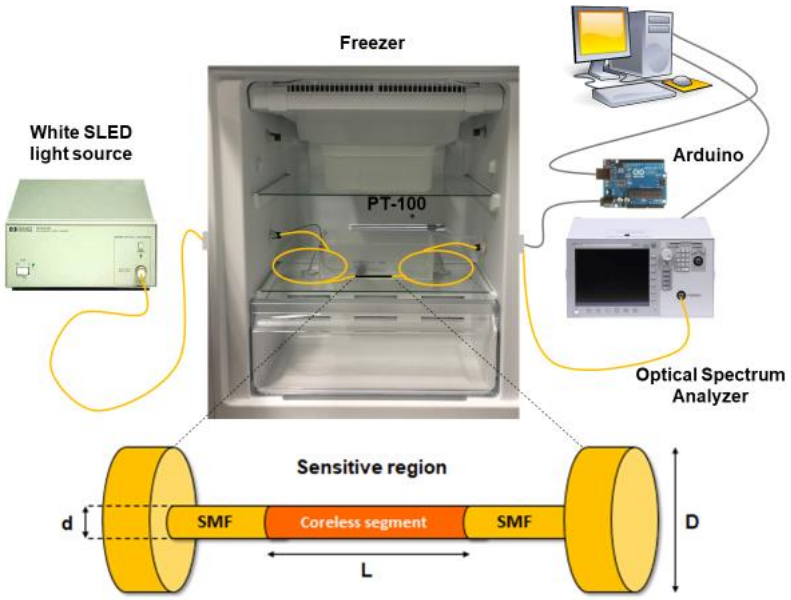

"Fig. 1. Experimental set-up to perform the ice detection".

3. Results and discussion

First, a theoretical analysis with FIMMWAVE® and an experimental characterization were carried out as a function of the surrounding refractive index (SRI). For this purpose, an original SMS structure of 58 mm coreless segment-length and the proposed E-SMS structure were compared. Fig. 2a shows the spectra for both structures. In the case of the original SMS structure, the self-image band located at 1550 nm was used for the detection of SRI, whereas any of the attenuation bands showing up in the E-SMS could be used to characterize the behavior of the new structure. Several solutions of glycerol in water were prepared, in order to cover a 0% - 60% v/v percentages, what means a SRI range from 1.321 to 1.408 RIU. The optical fiber structures were immersed in these solutions and the spectral responses were collected in order to analyze their behavior.

For the sake of comparison, the results for 125 and 30 micron-diameter E-SMS are analyzed in Fig. 2b. As it can be observed, numerical and experimental results are similar in the refractive index range analyzed. In the case of the 125 micron-diameter SMS, the overall estimated sensitivity is 183 nm/RIU, whereas the sensitivity for the 30 micron-diameter E-SMS are is 776 nm/RIU. This involves a 4.24-fold improvement with respect to the 125 micron-diameter SMS.

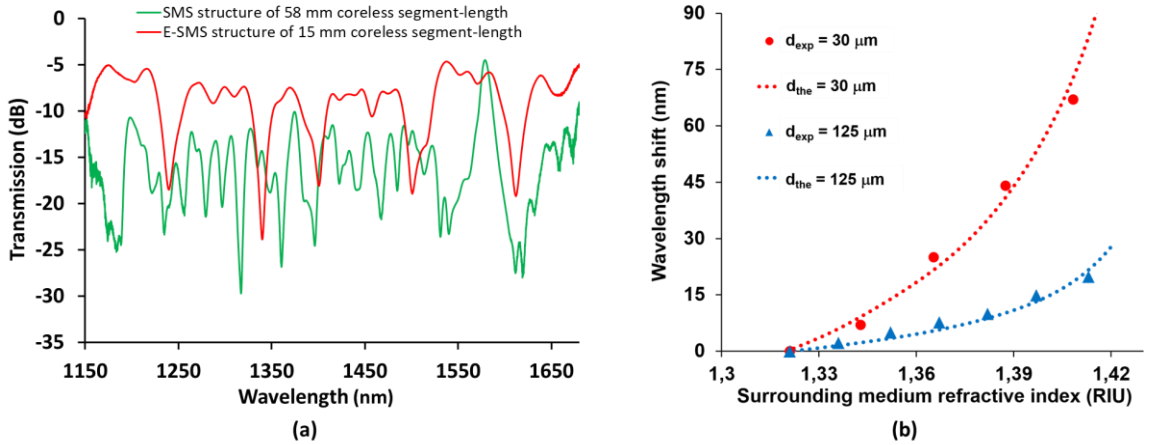

"Fig. 2. (a) Original spectra of the 58 mm coreless segment-length SMS and the proposed E-SMS structure. (b) SRI sensitivity of the SMS-based interferometers (discrete points and dashed lines represent experimental and theoretical results respectively).

Once the sensitivity to SRI is analyzed, the next step is to monitor the ice formation inside the freezer. The goal is to observe how the generated attenuation bands shift as a function of the decreasing water temperature and to check what happens when the water freezes, by means of the detection of the SRI due to the liquid-to-

solid state change. Hypothetically, there will be a refractive index change to lower values, what should be monitored as a blue-shift in wavelength. To analyze these results, we will focus on one of the attenuation bands of the spectrum and monitor its evolution over time.

The results are plotted in Fig. 3. Here, two freeze-unfreeze cycles are monitored within the climatic chamber. Each complete cycle takes a whole day. The green curve corresponds to the temperature measured with the Pt100 immersed in water during the experiment. Since the freezer is capable of performing a progressive process, it can be observed that the freezing takes more or less an hour and a half to decrease from 21 to -21˚C. After that, the freezer keeps freezing for an hour. Then, it is disconnected from the electrical network, and the unfreezing process takes place for 12 hours, what is a way to check the quality of the internal chamber when preserving the temperature.

Superimposed to this electrical measurement, the wavelength evolution of the previous mentioned attenuation band is shown in red. A total of 12.75 nm-shift is registered and several stages can be distinguished.

During the first freezing process, the optical signal follows the decreasing temperature until reaching -5ºC by means of temperature sensitivity. At this point, a sudden decrease is registered, from 1231 to 1226.5 nm, while the temperature keeps decreasing progressively to -21ºC. The reason for this behavior is that it gets to a point where all the water has frozen and the SRI outside the fiber is 1.308, according to [12]. Therefore, the sensitivity of the device to SRI is higher than the sensitivity to temperature and that is why this fast decrease occurs. In fact, it can be observed that the optical response is quite stabilized even when the freezer has been disconnected from the electrical network and the temperature increases to the 0ºC - 5ºC range. In this second stage, when ice starts to fuse progressively, the SRI rises from 1.308 to that of the liquid water and that is why a 8 nm red-shift of the attenuation band is observed. Finally, once all the water is in liquid state, the sensitivity to temperature acts again, red-shifting the central wavelength of the interferometric band 4 nm more until reaching the original temperature (+21ºC). The same behavior can be observed for both cycles.

The previous reasoning is reflected spectrally in Fig. 4a. We consider the attenuation band located at the shortest wavelength in the E-SMS spectrum obtained in Fig. 1a. This band is centered at 1239 nm (Fig. 4a). Following the evolution of this central wavelength as a function of time for every 5ºC increment, it is possible to analyze what happens at specific points of the process and then induce the sensitivity of the presented device. In this sense, Fig. 4b represents the evolution of the wavelength shift as a function of the freezing – unfreezing process. The different stages previously analyzed can be observed in the three areas of the graph along the total 12.75 nm wavelength shift. They correspond to temperature ranges from -21ºC to -11ºC, from -11ºC to 16ºC and from 16 to 21ºC. Between -21ºC and -11ºC, the wavelength remains quite stable, since the water is frozen and the SRI is 1.308 RIU all the time. In the region from 16 to 21 ºC an average sensitivity of 438 pm/ºC is registered. In the middle between both regions, it takes time for the water to either freeze or fuse. In the case of freezing, only when most of the water is frozen the refractive index suddenly decreases to 1.308 RIU and the attenuation band blue-shifts with an average sensitivity of 636 pm/ºC (0ºC – -10ºC interval). In the case of unfreezing, only when most of the water is sufficiently fused the refractive index progressively increases to 1.321 RIU and the attenuation band red-shifts (5ºC – 16ºC) with a sensitivity of 1 nm/ºC. Moreover, when freezing, since the cooling process is induced, the sensor response is more progressive, although it is possible to detect the moment when all the water is transformed into ice. After disconnecting, the heating process is more natural, and the sensor response when detecting the solid-to-liquid change of state is more drastic because it reacts only when natural physical conditions are adequate.

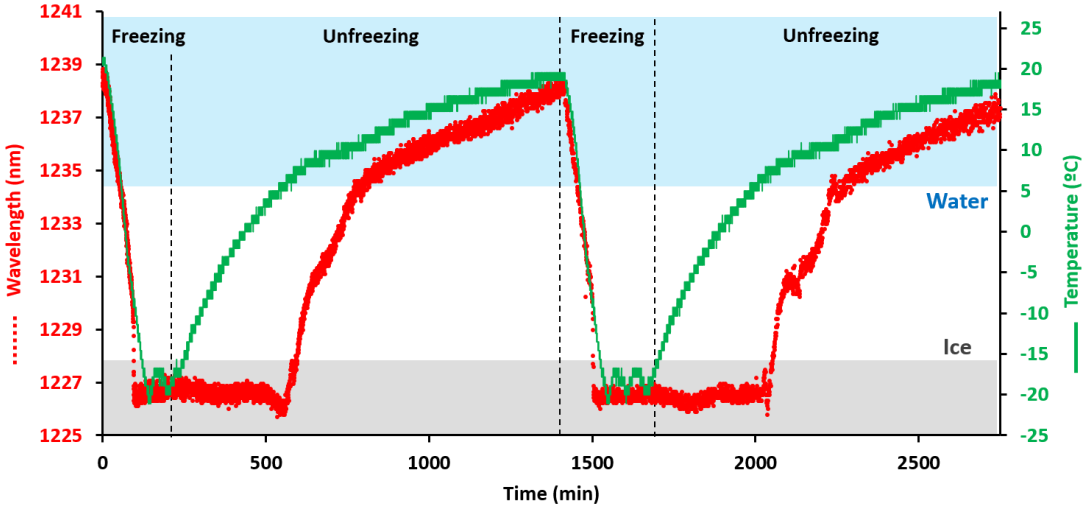

"Fig. 3. Temperature vs wavelength comparative evolution. Both water and ice states can be distinguished as well as the transitions between them."

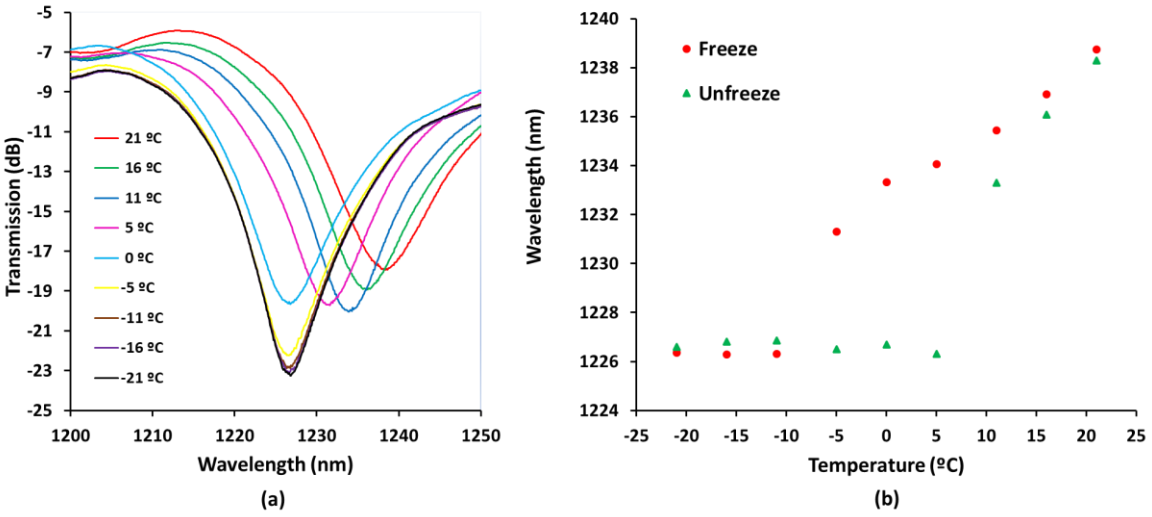

"Fig. 4. (a) Wavelength shift of the attenuation band analyzed. (b) Sensibility evolution during the freezing-unfreezing processes."

To conclude. it can be said that a basic fiber-optic interferometer has been characterized to detect the ice formation. The electronic and optical curves corroborate that there is a moment when the refractive index outside the fiber-optic structure changes suddenly and that is the key element to detect ice formation. With these results, a new research line is open in the detection of ice formation by means of simple and easy-to-handle fiber-optic sensors.

4. Acknowledgements

This work was supported by the Spanish Ministry of Education and Science-FEDER TEC2016-78047. The authors would like to thank BSH Electrodomésticos España S.A. for providing the necessary freezer to carry out the experiments.

5. References

[1] Y. Zheng, T. Lang, T. Shen, C. Shen, "Simple immunoglobulin G sensor based on thin core single-mode fiber", Optical Fiber Technology, Volume 41, 2018, pp. 104-108.

[2] Chen, Y.; Lin, Y.B.; Li, C.; Li, Q.Q. Fiber bragg grating strain sensor applied in security monitoring of road tunnel structure. In Advances in Mechanical and Electronic Engineering; Springer: Berlin/Heidelberg, Germany, 2012; pp. 323–328.

[3] Y. Geng, X. Li, X. Tan, Y. Deng, Y. Yu, High-sensitivity mach-zehnder interferometric temperature fiber sensor based on a waist-enlarged fusion bitaper, IEEE Sensors J. 11 (November (11)) (2011); pp. 2891–2894.

[4] Liquid-Infused Nanostructured Surfaces with Extreme Anti-Ice and Anti-Frost Performance
Philseok Kim, Tak-Sing Wong, Jack Alvarenga, Michael J. Kreder, Wilmer E. Adorno-Martinez, and Joanna Aizenberg
ACS Nano 2012 6 (8), pp. 6569-6577.

[5] Jackson, D., Liao, J., and Severson, J., "An Assessment of Goodrich Ice Detector Performance in Various Icing Conditions," SAE Technical Paper 2003-01-2115, 2003, https://doi.org/10.4271/2003-01-2115.

[6] Vibration measuring instrumentation - Fundamental requirements and verification. **¡Error! Referencia de hipervínculo no válida.**http://www.din.de/en/wdc-beuth:din21:2880513.

[7] Y. Lopez-Dieguez, J.M. Estudillo-Ayala, D. Jauregui-Vazquez, J.M. Sierra-Hernandez, L.A. Herrera-Piad, J.M. Cruz-Duarte, J.C. Hernandez-Garcia, R. Rojas-Laguna, Multi-mode all Fiber Interferometer based on Fabry-Perot Multi-cavity and its Temperature Response, In Optik - International Journal for Light and Electron Optics, Volume 147 (2017), pp. 232-239, ISSN 0030-4026.

[8] T. Yuan, X. Yang, Z. Liu, J. Yang, S. Li, D. Kong, X. Qi, W. Yu, Q. Long, and L. Yuan, "Optofluidic in-fiber interferometer based on hollow optical fiber with two cores," Opt. Express 25 (2017), pp. 18205-18215.

[9] Bo Dong, Member, IEEE, Member, OSA, Zhanyu Shen, Changyuan Yu, and Yixin Wang. Modal Excitations in Fully and Partially Ethanol-Filled Photonic Bandgap Fibers and Their Applications as Fiber Sensors. JOURNAL OF LIGHTWAVE TECHNOLOGY, VOL. 34, NO. 16, (2016), pp. 3853-3858.

[10] I. Del Villar, A.B. Socorro, J.M. Corres, F.J. Arregui, I.R. Matias, "Refractometric sensors based on multimode interference in a thin-film coated single-mode–multimode–single-mode structure with reflection configuration,", Appl. Opt., Vol. 53 (18) (2014), pp. 3913–3919.

[11] Yamile Cardona-Maya, Abian B. Socorro, Ignacio Del Villar, José Luis Cruz, Jesus M. Corres, Juan F. Botero-Cadavid,
Label-free wavelength and phase detection based SMS fiber immunosensors optimized with cladding etching, Sensors and Actuators B: Chemical, Volume 265 (2018), pp. 10-19, ISSN 0925-4005.

[12] S. Warren, "Optical constants of ice from the ultraviolet to the microwave," Appl. Opt. 23, pp. 1206-1225 (1984).